Analysis of Pulsed Gas Metal Arc Welding (P-GMAW) Heat Input on UNS-S32101 Lean Duplex Stainless Steel

by

Roger Carter

A Thesis Presented in Partial Fulfillment
of the Requirements for the Degree
Master of Science in Technology

Approved April 2011 by the
Graduate Supervisory Committee:

Bradley Rogers, Chair
Jerry Gintz
Trian Georgeou

ARIZONA STATE UNIVERSITY

May 2012

ABSTRACT

This report presents the effects and analysis of the effects of Pulsed-Gas Metal Arc Welding's (P-GMAW) on Lean Duplex stainless steel. Although the welding of Duplex and Super Duplex Stainless steels have been well documented in both the laboratory and construction industry, the use of Lean Duplex has not. The purpose for conducting this research is to ensure that the correct Ferrite-Austenite phase balance along with the correct welding procedures are used in the creation of reactor cores for new construction nuclear power generation stations. In this project the effects of Lincoln Electrics ER-2209 GMAW wire are studied. Suggestions and improvements to the welding process are then proposed in order to increase the weldability, strength, gas selection, and ferrite count. The weldability will be measured using X-Ray photography in order to determine if any inclusions, lack of fusion, or voids are found post welding, along with welder feedback. The ferritic point count method in accordance with ASTM A562-08, is employed so that the amount of ferrite and austenite can be calculated in the same manor that is currently being used in industry. These will then be correlated to the tensile strength and impact toughness in the heat-affected zone (HAZ) of the weld based on the ASTM A923 testing method.

DEDICATION

I would like to dedicate my Masters thesis to my father, Roger C. Carter III, with out his guidance, love, and constant encouragement I would not be the man I am today. I love you, Dad and this one's is for you.

ACKNOWLEDGMENTS

I would like to thank my committee members Dr. Bradley Rogers, Professor Trian Georgeou, and Professor Jerry Gintz for their efforts in helping me complete my degree at a distance.

I would also like to thank my supervisors and colleagues at The Shaw Group, Shane Finland, Mike Phillips, and Bryan Toth; it is because of all of your expertise in the field of welding that I have been able to complete my degree. I consider the work that is being performed at Shaw in Welding Technology and Services to be an invaluable asset to not only the nuclear industry but the welding community at large.

Special thanks are also given to Brian Hart and Elliott Ashe at Lincoln Electric for their continued support in the P-GMAW system and helping aiding me in collecting and interpreting my data.

Lastly, I would also like to thank the entire staff at Element Materials Technologies for their material testing services.

TABLE OF CONTENTS

Page

Page

CHAPTER

LIST OF TABLES

LIST OF FIGURES

Chapter 1

INTRODUCTION

1.1 Background

The use of stainless steels in the energy industry has been extensive and well-documented. However, with the emergence of new nuclear plant construction regulators, designers, and material manufacturers, we are forced to make improvements to this material. Lean duplex has emerged as a great candidate to meet these new rules but little is know about how this material reacts to pulsed-gas metal arc welding (P-GMAW).

The following testing was conducted with the assistance of The Shaw Group Inc. (Shaw) in order to perform all of its process qualification record (PQR) testing. Shaw performs various welding tests to qualify the weld strength of particular joint geometries, positions, filler materials, and welding processes in accordance to the standards set out by the American Society for Testing and Materials (ASTM) A370-09a Standard Test Methods and Definitions for Mechanical Testing of Steel Products, ASTM A 923 – 08 Standard Test Methods for Detecting Detrimental Intermetallic Phase in Duplex Austenitic/Ferritic Stainless Steels, ASTM E 562 -08 Standard Test Method for Determining Fraction by Systematic Manual Point Count, American Welding Society (AWS) D1.1: 2000 Structural Welding Code – Steel, AWS D1.6: 1999 Structural Welding Code – Stainless Steel and The Westinghouse Electric Company (Westinghouse).

1.2 Statement of Problem

The purpose of this research was to determine how Lincoln Electrics Pulsed-Gas Metal Arc Welding (P-GMAW) process, along with their ER2209 welding wire, would affect the ferrite-austenite phase balance of UNS S32101. The knowledge gained from this study will benefit the nuclear and welding communities in several ways:

- Improves' understanding of how lean duplexes react to the P-GMAW process.
- Prevent overly stringent material qualifications being assigned from government and other regulatory bodies of future nuclear projects
- Aid manufacturers of P-GMAW equipment and welding wire by furthering their understanding of where improvements need to be focused
- Ensure that correct welding techniques and procedures are used in the field

The specific goals of this study were to:

- Determine how variations in the P-GMAW waveform affect the heat input (kJ/inch) and the ferrite-austenite phase balance of UNS-S32101, using ASTM E 562-08 Standard Test Method for Determining Volume Fraction by Systematic Manual Point Count.
- Identify cavities, inclusions, and others modes of failure through X-Ray examinations in accordance with AWS D1.1: 2000 Structural Welding Code – Steel.

- Perform charpy impact testing at -40º Fahrenheit and tensile testing shall be performed in accordance with Westinghouse Document Number APP-VW20-Z0-023 Welding Specifications for ASTM A240 UNS S32101 Duplex Stainless Steel Plate, ASTM A 923-08 Standard Test Methods for Detecting Detrimental Intermetallic Phase in Duplex Austenitic/Ferritic Stainless Steels, and ASTM A370-09a Standard Test Methods and Definitions for Mechanical Testing of Steel Products.
- All visual examinations American Welding Society's (AWS) Section D1.6: 1999 Structural Welding Code – Stainless Steel, along with standards set out by Westinghouse.

1.3 Scope

This study was created in order to understand how the material properties changed in UNS-S32101 stainless steel after being welded using various frequencies in the P-GMAW system. The Shaw Group (Shaw) provided the facilities and equipment for this study, due to their need for a greater understanding of lean duplexes stainless steels.

The scope of this study can be seen in Figure 1.1. Test plates were welded using the P-GMAW process, visually examined for cracks, weld penetration, and sharp edges on the beads. Then the coupons were sent to Element Material Technologies for X-Ray examination where they were visually examined for slag inclusions, voids, and weld penetration. They were then cut in to test samples for ferrite-austenite point count, tensile testing, and charpy testing. The heat input

(kJ/inch) was calculated using data gathered from the Lincoln Electric Power Wave Software and graphs were created comparing showing the different frequencies that were used and how heat input changed per the variance in frequency.

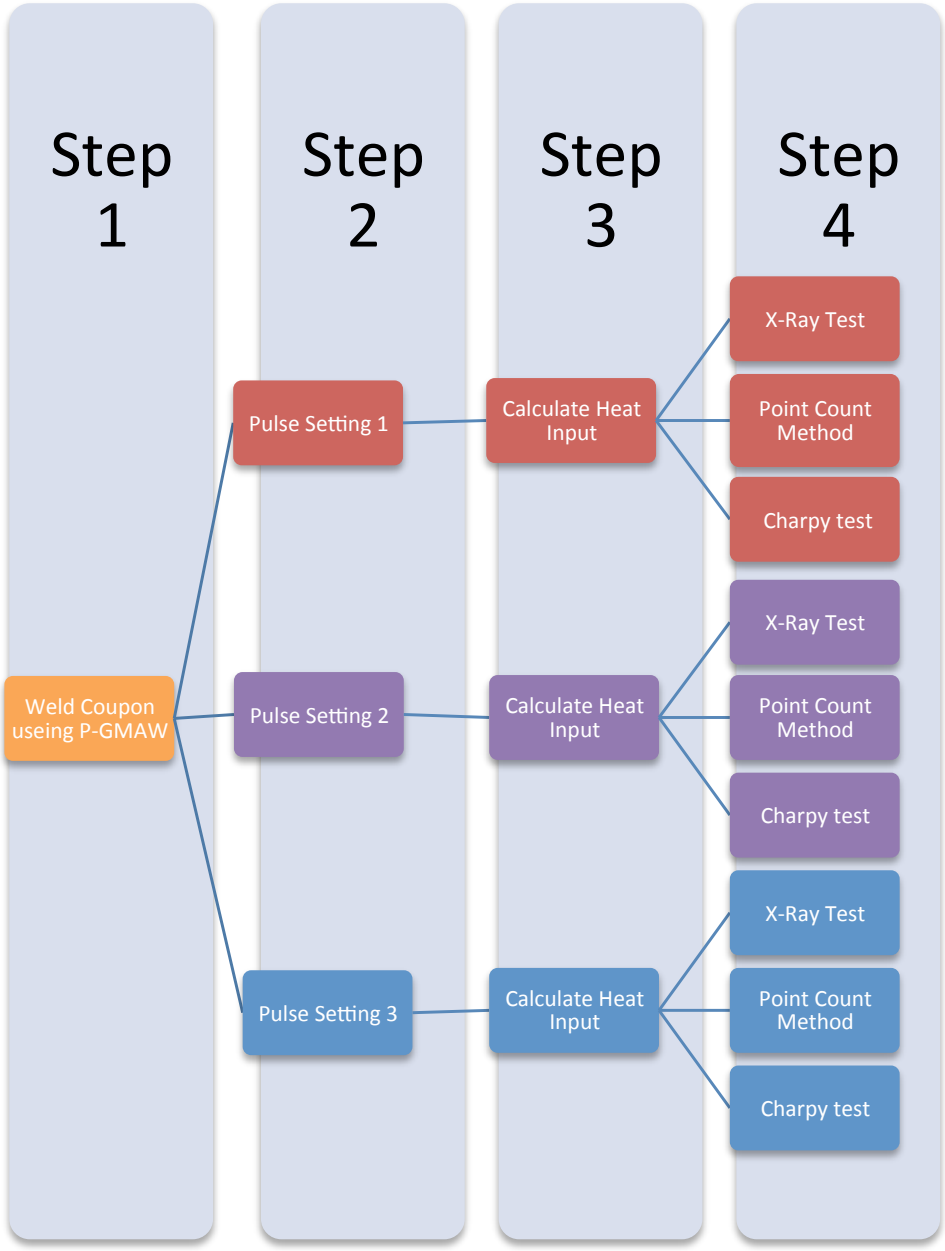

Figure 1.1: Illustration of Work Flow

Chapter 2

Literature Review

2.1 Literature Survey

This chapter introduces a literature overview of the pulsed-gas metal arc welding (P-GMAW) process, along with a detailed report of the equipment used for testing. At Encompass Machines Incorporated where the testing for this study was performed, the Welding Technology and Services Department employees at The Shaw Group (Shaw) conduct welder certifications and procedure qualification record (PQR) testing for all of Shaw's welding needs. These facilities include a material storage area, office space for engineering personnel, welding stations, and robot welding testing fixtures. All of this is necessary to comply with the standards set out by American Society of Testing and Materials (ASTM), American Welding Society (AWS), and Westinghouse Electric Company (Westinghouse) for the creation of the AP1000 Nuclear Power Generation Stations. In order to meet the requirements set out by these governing bodies, test coupons are welded using a range of welding parameters, allowing welders to personalize settings for their particular style.

2.2 Material Properties of UNS-S32101 Lean Duplex

The term "lean" is derived from the low alloying necessary to create the material along with the relatively low 1.5% nickel content found. The low nickel content would normally generate a high level of austenite, but this has been countered by adding 0.20% nitrogen and 4.00% manganese. S32101 is

manufactured in accordance with American Society for Testing of Materials (ASTM) specification A240 “Chromium and Chromium-Nickel Stainless Steel Plate, Sheet, and Strip for Pressure Vessels and for General Applications”. Table 2.1 shows the chemical composition of the material used in this study. The benefits that come with using a Lean Duplex material versus other types of Duplex are higher strength, excellent resistance to chloride stress corrosion cracking (SCC), and improved weldability (Sieurin, Sandstom & Westin).

Table 2.1 Chemical composition, of UNS-S32101 Lean Duplex in %

Alloy	Min	Max
Chromium (Cr)	21.0	22.0
Nickel (Ni)	1.35	1.70
Manganese (Mn)	4.00	6.00
Molybdenum (Mo)	0.10	0.80
Nitrogen (N)	0.20	0.25
Carbon (C)	—	0.040
Silicon (Si)	—	1.00
Copper (Cu)	0.10	0.80
Phosphorus (P)	—	0.040
Sulfur (S)	—	0.030
Iron (Fe)	Balance	

The strength of this material is comparable to UNS-S32205, as can be seen in Table 2.2, where the only differences between the two materials was a 1 ksi ultimate tensile strength, 5% difference in Elongation and the 3 unit difference in Brinell hardness (*Ldx 2101 fabrication*).

Table 2.2 Tensile Properties of Cold Rolled Plate ¼ Inch Thick

	Strength, ksi (Min)	Strength, ksi (Min)	Percent (Min)	Brinell (Max)
LDX 2101	94	65	30	290
304/304L	75	30	40	201
316/316L	75	30	40	217
2205	95	65	25	293
2304	87	58	25	290
AL 2003™	95	65	25	293

Due to the lightweight nature of S32101, it creates a lower cost of manufacture because a thinner gauge of material can be utilized along with reducing the transportation and shipping costs (*Ldx 2102 fabrication*).

Often times, 300 series stainless steels are used for their good corrosion resistance, with the onset of pitting and stress corrosion cracking being one of the most common reasons for stainless steel equipment failure see Figure 2.1 and Figure 2.2.

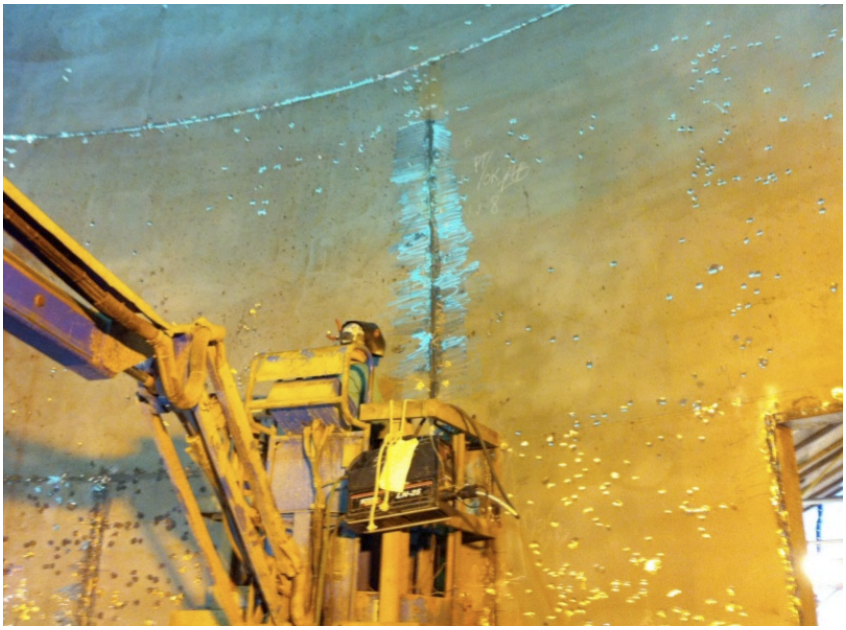

Figure 2.1 Image of Pitting and Stress Corrosion Cracking

Figure 2.2 Magnified Image of Pitting and Stress Corrosion Cracking

Figure 2.3 illustrates the corrosion resistance possible with using UNS-S32101 (*Ldx 2101 fabrication*). Stress corrosion cracking is usually caused by chlorides produced during the manufacturing process or are found externally on piping located near coastal waterways (*Practical Guidelines*, 2009).

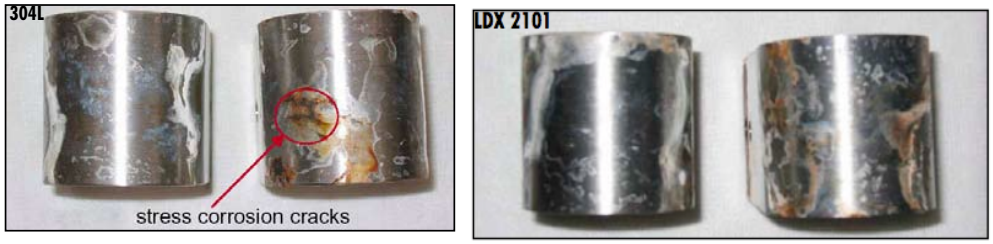

Figure 2.3: Corrosion Test Performed Using ASTM C692 after 672 Hours at 212^{O} Fahrenheit

2.3. Pulsed-Gas Metal Arc Welding (P-GMAW)

Because of the high deposition rates that are associated with GMAW, it makes it the ideal process for welding thick materials. However, in the past, this

process has been position limited because it has been a gravity-delivered system. By controlling the way in which the filler material is transferred to the weld pool, spatter, arc stability, weld quality, and multiple welding positions can be utilized.

The traditional GMAW process works by creating an arc through the electrode or filler wire (positive connection) with the base material (negatively grounded) using direct current. This arc generates the necessary amount of heat to melt the base material while also melting the filler material (Norrish, 2006). As a droplet forms, if falls off of the filler material depositing itself in the weld pool, this is called free-flight transfer. Welding can be performed by use of continuous current in the short-circuit mode or by the use of a pulsed current.

P-GMAW uses a spray mode of metal transfer allowing for a lower mean current to be utilized, which helps in preventing distortion (Ghosh, Gupta & Randhawa). The process works by having a low background current allowing an arc to be maintained while also creating a droplet on the tip of the electrode. The droplet is 'forced' from the electrode tip by the use of a high current pulse as can be seen in Figure 2.4 (*Practical Guidelines*, 2009). This high current creates a large electromagnetic force making the droplet become constricted on the electrode tip, where it then releases from the tip and travels across the arc gap to the base material.

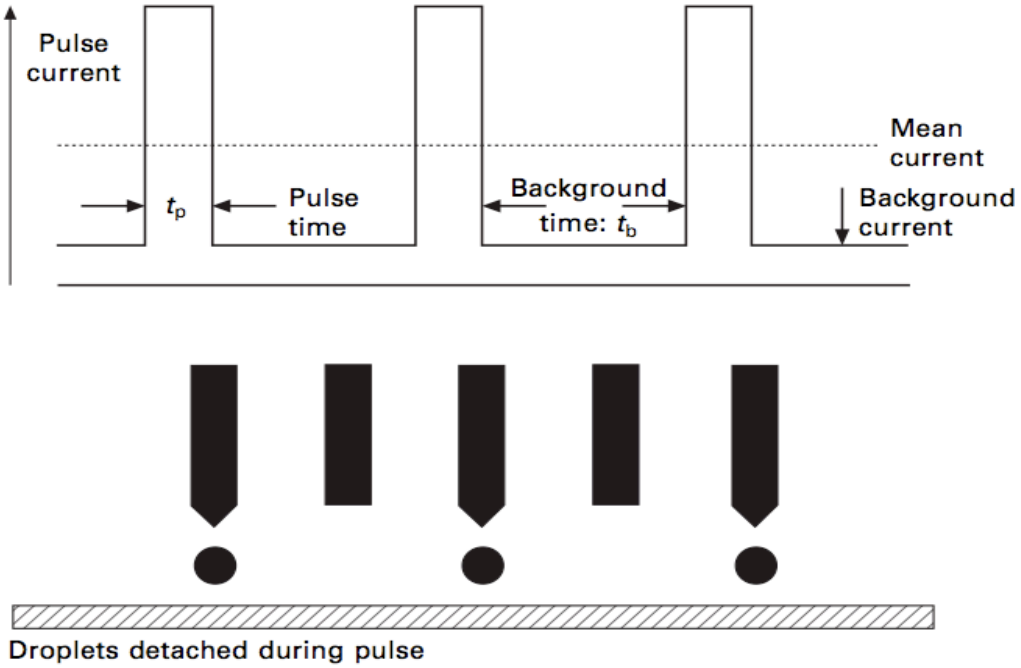

Figure 2.4: Illustration of how the P-GMAW is Performed

This duality in processes creates both a globular and a projected spray welding type. The point at which these two processes differ is called the transition current and differs depending on wire type, wire diameter, composition of base material and the shielding gas.

When the current is lower than the transition current, the welding characteristics are more globular, generating large droplets and low transfer rates. When the base current is increased, smaller droplets are generated, and the time between pulses consequently shortens. This also has the tendency to create multiple droplets per a pulse (Ghosh, Gupta & Randhawa).

As the current continues to rise and becomes larger than the transition current, the droplet size becomes even smaller, until the droplets are the same size as the wire diameter. In order to achieve this, very high frequencies are required.

This consequently requires very large currents to get such small droplets, thereby generating bigger heat affected zones thru increased weld pool diameter. In addition, the droplets are projected axially through the arc with a significant amount of force.

The background current, pulse current, pulse time, background time, and pulse frequency create the velocity necessary to propel the droplet from the electrode tip with enough force to defy gravity. All of these factors also aid in framing the desired weld pool through droplet size and penetration temperature. This allows the P-GMAW to have higher filler metal deposition rates, while also minimizing the heat input (Norrish, 2006).

2.4 Heat Input Calculations

Heat input can be defined as the amount of energy (Joules) put into a piece of material over a given distance (inches). Table 2.3 shows the traditional method of calculating the heat input (WEC, 2010).

Calculation 2.1: Traditional Method of Calculating Heat Input

$$\frac{\text{Amps (A)} * \text{Volts (V)} * 60}{\text{Travel Speed (inches/minute)}} = \frac{\text{Joule}}{\text{Inch}}$$

The Lincoln Electric Power Wave® S350 P-GMAW system that was used for this study, has a built-in data acquisition system that continuously calculates the voltage, amperage, and kilo joules of energy (True Energy™) put into the weld. This system samples voltage and amperage values at a rate of up to 120,000 times per second (120 kHz) and uses those values to calculate the True Energy™ (*Nextweld: True energy,* 2009).

Raw Data				Integrating under the curve using Trapezoids:		
Time	Raw Volts	Raw Current		Actual Volts	Actual Amps	Calculated kJ
5.83	22.97	69.53		0.000370	0.001094	0.000027
5.83	22.81	67.97		0.000428	0.001248	0.000026
5.83	23.44	68.75		0.000495	0.001375	0.000027

Table 2.4 Integration of Raw Data to Actual Data

Since both the voltage and amperage are changing continuously due to the pulsing system along with accounting for variance in contact tip to work distance, the true voltage and amperage readings can only be attained once there respective sign waves have been integrated using the trapezoidal integration method as seen in Table 2.5 (*Process: Pulsed spray*, 2004). An example of a voltage square wave and amperage sign wave can be seen in Figures 2.5 and 2.6.

It can be seen in Figure 2.6 that the peak voltage is flat with a very long but relatively high background voltage. This square wave shave is hugely different when visually examining Figure 2.7, with its much more pronounced sign wave curve and relatively lower background current.

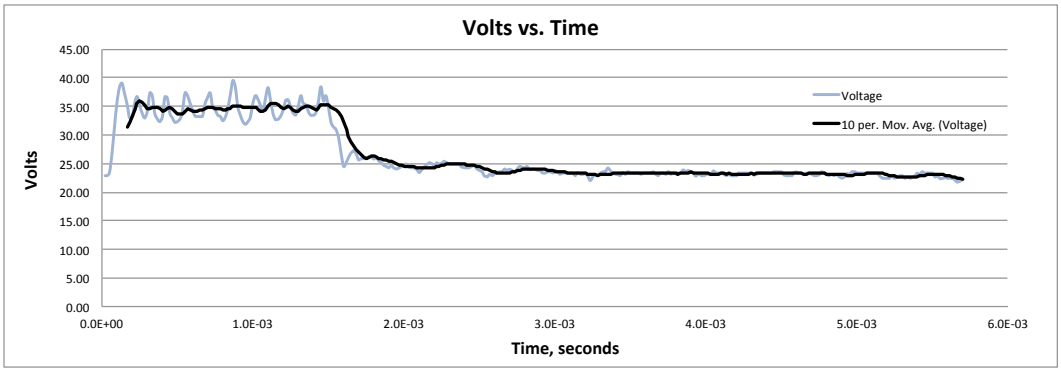

Figure 2.6 Volts vs. Time Graph

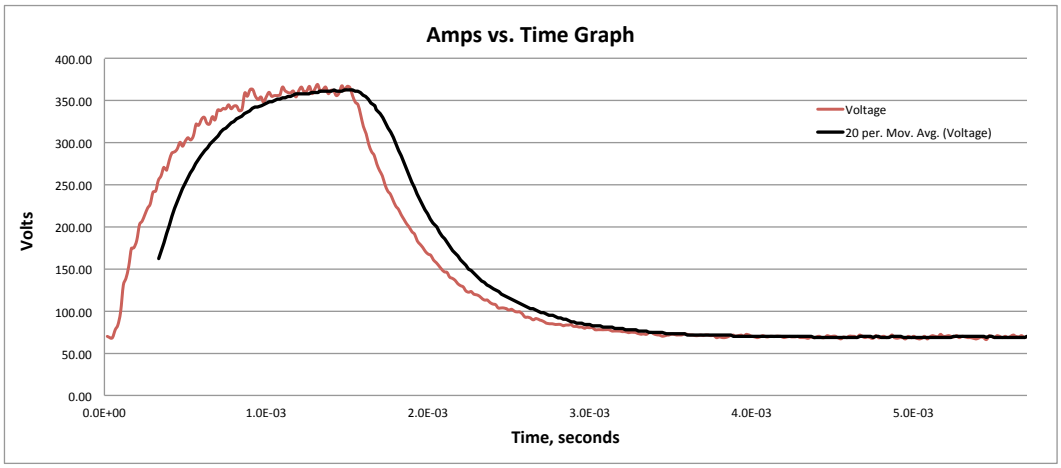

Figure 2.7 Amps vs. Time graph

In order to calculate and display the True Energy™, the Lincoln Electric Power Wave® S350 multiplies the "Raw Volts" against the "Raw Current" and divides by 1,000 to attain kilowatts as can be seen in the equation outlined in Table 2.5.

Calculation 2.2: Calculating Power (KW)

$$\frac{V_R * I_R}{1000} = kW$$

In Table 2.5 the raw current is represented by V_R, with the raw current being denoted as I_R, and the kilowatts shown as kW.

The newly-created kilowatts value is then multiplied by the amount of time that has passed since the last sample reading. By continually multiplying and adding these values over an entire sign wave, this will lead to the "Summation of kJ per Wave" value shown in Table 2.6. The amount of energy emitted for each wave can be can be summed up then multiplied by the number of waves that occur per a second, in order to determine the "Kilojoules / Second"

value seen in Table 2.6. This value will continually increase as long as welding is occurring. Once the welder has completed the desired weld length, the system displays the True Energy™, or kilojoules.

Table 2.6: Table Outlining the True Energy™ Calculation Process

Summation of Volts per Wave:	Summation of Amps per Wave	Summation of kJ per Wave	Volts / Second	Amps / Second	Kilo Joules / Second	True Energy	Calculated Heat Input
0.1508	0.8744	0.0265	26.5	153.4	4.64	357.3	29.77

By taking the True Energy™ value and dividing it by the welded distance traveled, the heat input value can be calculated, see Table 2.7. This methodology is the preferred way of calculating the actual amount of energy being placed into the weld because of the high sample rate. The traditional method of determining the heat input is designed around using a standard GMAW process. This is not to say that the values calculated from the traditional method are wrong, but must be interpreted with this in mind.

Calculation 2.3: Calculating Heat Input Using True Energy™

$$\frac{\text{True Energy}^{TM}\text{ (Joules)}}{\text{Welded Distance, inches } (d_i)} = \frac{\text{Joules}}{\text{inch}}$$

There are other factors that may skew the True Energy Value™ reading such as arc efficiency, welding cable length, or inductance caused by wound-welding cable. Although these issues do exist, they are only factored in when welding an object a great distance from the welding machine.

2.5 American Welding Society D1.1: 2000 radiographic examination

The purpose of conducting an X-Ray examination is to determine if the material being used for testing contains any voids, cracks, or slag inclusions

through non destructive testing methods. This visual examination process is a significant determinant of whether or not a specimen was welded together properly.

Voids are indicated on radiographic film by black or grey figures against the white material. The density of the material is indicated by how white the image is, should objects appear to be greyer, the image indicates that the density has changed from that of the base material (D1.1:2000, 2000).

2.6 Westinghouse Electric Company Inc. Welding Specification for ASTM A240 UNS S32101 Duplex Stainless Steel Plate:

This document outlines the parameters The Westinghouse Electric Company (Westinghouse), wishes to have the group AP1000 nuclear power plants constructed. The main focus of this document resides in impact toughness and percent of delta ferrite.

Westinghouse requires that a minimum of 20 ft-lbs at a temperature of -40ºF must be met for impact toughness in the weld metal and heat affected zone. This impact strength and temperature stem from the wide possible range of temperature that a AP1000 nuclear plant may be constructed in. They also outline a range of 35-65%, which Westinghouse deems acceptable amounts of ferrite to be found in the weld metal and heat affected zone.

2.7 ASTM A 923 – 08 Standard Test Method for Detecting Detrimental Intermetallic Phase in Duplex Austenitic/Ferritic Stainless Steels

During the duplex welding process, material exposed to temperatures between 600 and 1750^{o}F (320 to 955^{o}C) are susceptible to intermetallic phase

change. The rate at which this happens is relative to the material thickness, material density, torch angle, and welding speed. Both corrosion resistance and toughness can be affected during these phase changes (ASTM A 923 – 08, 2008). The point of conducting v-notch charpy testing is to determine the toughness of a material. Toughness is a materials ability to resist embrittlement and fast fracture in the presence of a notch or flaw. By implementing the correct heat treatment process and rapid cooling rates, lean duplex can retain the maximum amount of its original properties.

The Charpy Impact Test for Classification of Structures of Duplex Stainless Steel outlined in ASTM A 923 – 08, Section 1.5.2 Test Method B-Charpy Impact Test for Classification of Structures of Duplex Stainless Steels, Sections 8 thru Section 13 and also using ASTM A 370 Test Methods and Definitions and ASTM E23 outlines the industry standards for charpy testing of mill and cast products. This testing method was applied to base materials along with welded samples in order to maintain uniform testing parameters. Table 2.8 outlines the applicability and acceptance criteria for this testing method. Since S32101 is not an officially-recognized ASTM certified material yet, S32205 was used as the benchmark because it most closely relates than any of the other grades of material listed.

Table 2.8: Applicability and Acceptance Criteria for Charpy Impact Testing

Grade	Condition	Test Temperature	Minimum Impact Energy
S31803, S32205, J92205	Base Metal	-40°F (-40°C)	40 ft-lb (54 J)
	Heat Affected Zone	-40°F (-40°C)	40 ft-lb (54 J)
	Weld Metal	-40°F (-40°C)	40 ft-lb (54 J)
S32750	Base Metal	-40°F (-40°C)	40 ft-lb (54 J)
J93404	Base Metal	-50°F (-46°C)	40 ft-lb (54 J)

ASTM A 923 – 08 notes that the impact toughness of a transverse specimen from mill products of duplex is typically one half to two thirds of that of a longitudinal test piece, because of this, all specimens were set up in longitudinally.

2.5.2 ASTM E 562 – 08 Standard Test Method for Determining Volume Fraction by Systematic Manual Point Count:

The ASTM describes this process as a testing method that is "used to determine the volume fraction of constituents in an opaque specimen using a polished, planar cross section by the manual point count procedure" (*E562 Volm Fraction*, 2008). This particular method uses a transparent sheet of crosses laid out in either a grid or circular pattern at a magnification of 400 or 500x, to identify the amount of two different microstructural features of interest. Figure 2.5 illustrates two different grid patterns used for the point count method. The point fraction is the ratio of the point count of the microstructure of interest versus

the number of points that fall on non-points of interest, this is generally expressed as a percentage over a predetermined amount fields.

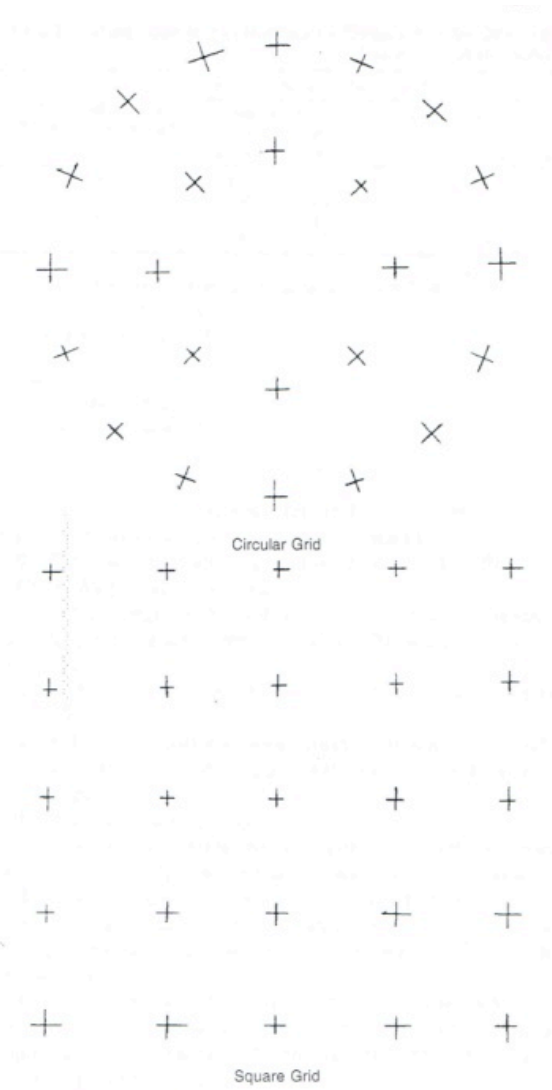

Figure 2.7 Illustration of Grid Patterns

Table 2.9 describes the calculation necessary to determine the interphase balance of ferrite to austenite ratio.

Calculation 2.4 Calculation to Determine the Ferrite to Austenite Ratio

$$P_P(i) = \frac{P_i}{P_T} * 100$$

$P_P(i)$ = Percentage of grid points observed on the i^{th} field
P_i = Total number of points in the test grid
P_T = Point count on the i^{th} field

2.5.3 ASTM A370 – 09 Standard Test Methods and Definitions for Mechanical Testing of Steel Products:

Tensile testing required by The Shaw Group (Shaw) and Westinghouse Electric Company (WEC) is used to determine the yield strength and elongation of welded samples using the prequalified joint geometry specified by American Welding Society (AWS) D1.1-2000.

Test specimens were prepared in accordance with Section 8.5.1 and Section 10 Sheet-Type Specimens. Dimensions for this specification can be seen in Figure 2.6. This was due to the fact that the base material was 0.500 inches in thickness and will qualify for base materials to be welded in the field from thickness ranging from 0.1875 – 1.000 inches.

Figure 2.8 Illustration of Dimensions Used for ½" Tensile Test Specimen

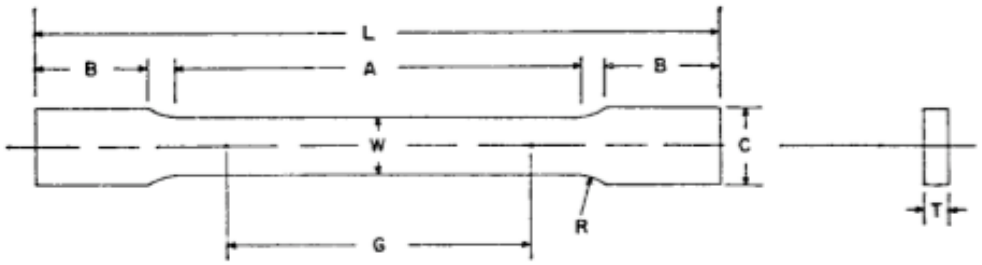

Standard Dimensions for Sheet-Type, 1/2 in. Tensile Test Specimen		
Location	Dimension, inches	Tolerances, inches
G - Gauge Length	2.000	+/- 0.005
W - Width	0.500	+/- 0.010
T - Thickness	Thickness of Material	
R - Radius of Fillet, min	0.500	+/- 0.005
L - Overall Length, min	8.000	+/- 0.010
A - Length of Reduced Section, min	2.250	-
B - Length of Grip Section, min	2.000	-
C - Width of Grip Section, Approximate	0.750	-

Chapter 3

WELDING CHARACTERISTICS AND DEFICIENCIES

3.1 Testing Fixture Description

This project was performed at The Shaw Group Inc.'s (Shaw's) research and development labs in Rock Hill, SC. The purpose of this facility is to perform process qualification reports (PQR's) for the Welding Technology and Services Group, so that new welding procedures can be used on new nuclear construction job sites such as VC Summer and Vogle Power Stations.

The experiments were performed in the 1G, flat position, using a ½ inch duplex coupon with a 304 stainless steel backer bar. The coupon was held in place by welding feet as can be seen in Figure 3.1. The fixture was made out of a ¾ inch and ¼ inch steel plate and was designed to prevent the coupon from bowing as much as possible. Excessive bowing can lead several problems including the weld joint closing up leaving the welder with a difficult to weld opening which could cause porosity, cracking, or lack of fusion; and example of excessive bowing can be seen in Figure 3.2.

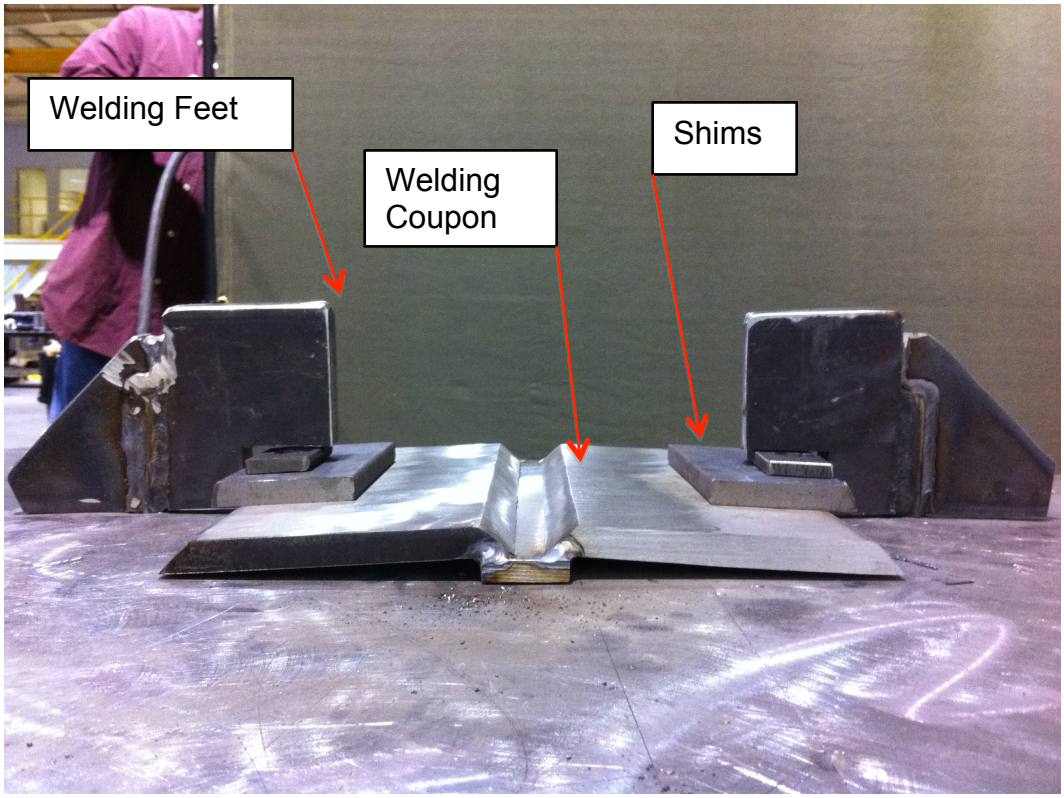

Figure 3.1 Image of Welded Coupon and Welding Feet

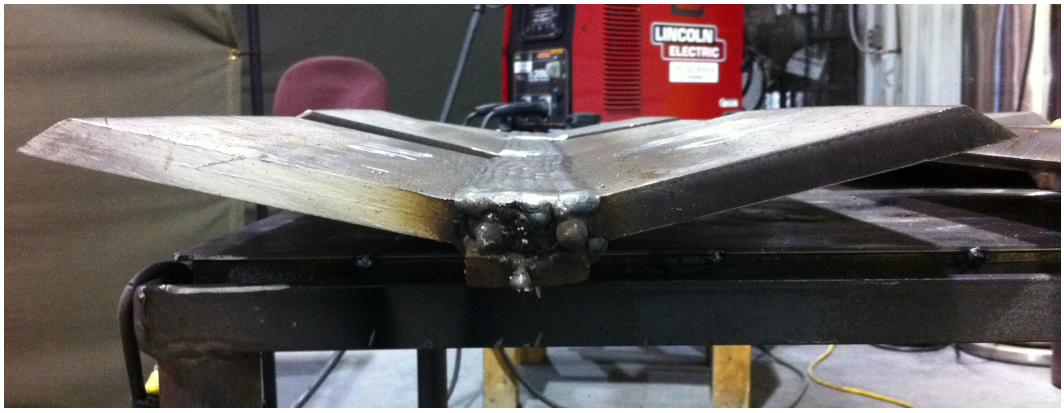

Figure 3.2 Image of Bowing

3.2 Welding Coupon Design

The coupons joint design, material and welding process stem from Westinghouse's design for the AP1000 nuclear power plant design, and Shaw's

use of a machine welding system. The joint geometry and material used for testing was a ½" thick piece of duplex stainless steel for the base material, with each side beveled to a 60º angle and was spaced to accommodate a 5/8 inch root gap. The 304 stainless steel backer bar that was used was 3/8 inch thick and tacked in place using the GMAW-P process. The gas used for all experiments was a tri-mix of 2.5% carbon dioxide, 38% helium, and 59.5% argon.

3.3 Experiments

The tests that were performed were conducted using the Lincoln Electric S350 GMAW-P system, with a Lincoln Electric ER2209 welding wire. Westinghouse specifies this wire for use on any duplex welding that occurs, so that corrosion resistance is not adversely affected during welding. A scrap piece of material was used before each test to properly set up each new frequency and to ensure that proper penetration would occur. Once welding began on each coupon the only variation that was allowed to occur would be wire feed speed.

The Lincoln Electric S350 has two different ways of setting up a GMAW-P process a traditional voltage setting and a "trim" setting. The traditional voltage setting increases the peak value seen in the waveform generating greater area underneath the curve, which gives the welder a larger amount of voltage to penetrate various thicknesses of base material. Trim, allows the welder to off-set the entire waveform, giving the welder more or less volts by evenly offsetting the entire waveform. By offsetting the waveform more evenly greater control voltage can be attained. The trim setting is a relative setting ranging from -10 to 10. If

the welder requires less voltage for a thinner piece of material then the operator would decrease the trim, and the reverse would occur for thicker materials. The trim offset is not the same for each different mode offered by Lincoln Electric so it was unknown what the variation in waveforms would be until Lincoln Electric unlocked the data for analysis. A total of four different modes were used to generate the different frequencies, a description of these different frequencies can be found in Table 3.1. In order to maintain uniformity in testing a two-bead root pass was standard for all coupons.

Table 3.1 Description of Modes and Settings Used for Experimentation

Experiment Number	Mode / Description	Volts / Trim Setting
TH-01	Mode 12, Steel 0.035 in. Wire	1.15
TH-02	Mode 16, Steel Verticle Up 0.035 in. Wire	28.0V
TH-03	Mode 155, Steel 0.035 in. Wire	0.95
TH-04	Mode 34, Stainless Steel 0.035 in. Wire	1.00

3.4 Data Collection

Interpass temperatures were taken using an Extech Inc. hand held laser pyrometer. Recorded temperatures were taken at the start of the weld and were kept below 500º Fahrenheit for all passes.

Heat input and weld time were collected from the digital display on the Lincoln Electric S350. The S350 samples voltage and amperage data at a rate of 120 kHz, which allows the machine to compensate voltage for amperage as contact tip to work distance changes. The Lincoln Electric Power Wave Software was used to record peak volts, peak amps, minimum volts, and minimum amps along with being used to take the sample graphical data.

Chapter 4

RESULTS & DISCUSSION

4.1 Amperage vs. Time Wave Form Analysis

The waveforms used for this experiment have been designated TH-01, TH-02, TH-03, and TH-04 as can be seen in Figure 4.1. Waveforms Th-01, TH-02, and TH-03 were originally designed by Lincoln Electric for welding of steels, but were used in this experiment to generate the necessary variation in waveform.

Major variations in the ramp up rate, peak amperage, time at peak amperage, drop off rate, and frequency are noticeable. This shows that if waveform modification is to have an effect on tensile properties, impact strength, and delta ferrite it should be noticeable.

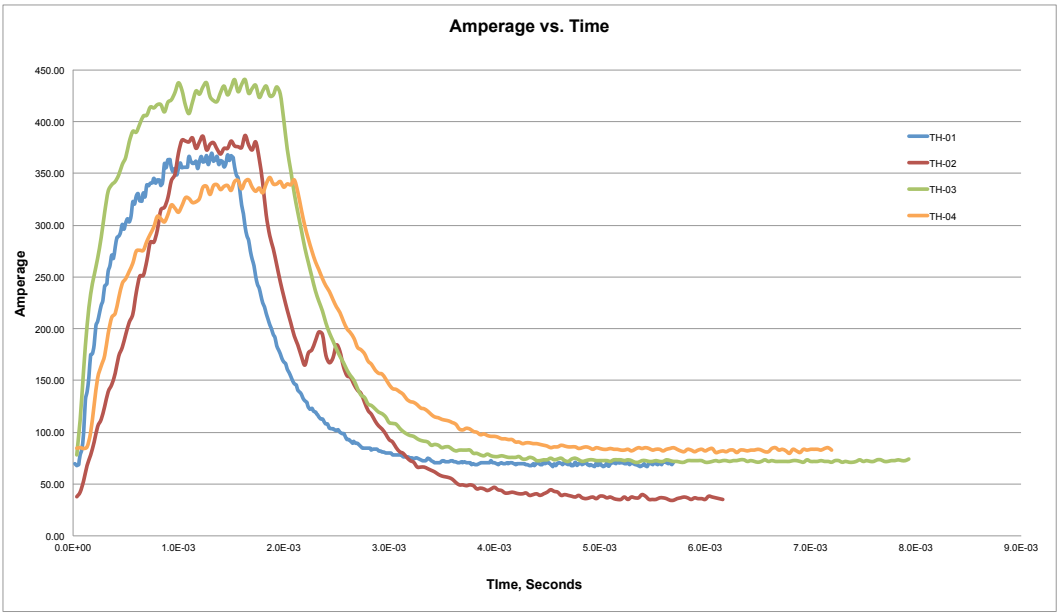

Figure 4.1 Amperage vs. Time Waveforms

Experiment TH-04 is specifically designed to weld stainless steels, and is the waveform most often used for welding duplex. TH-04 will be considered the baseline against which all tests will be compared to.

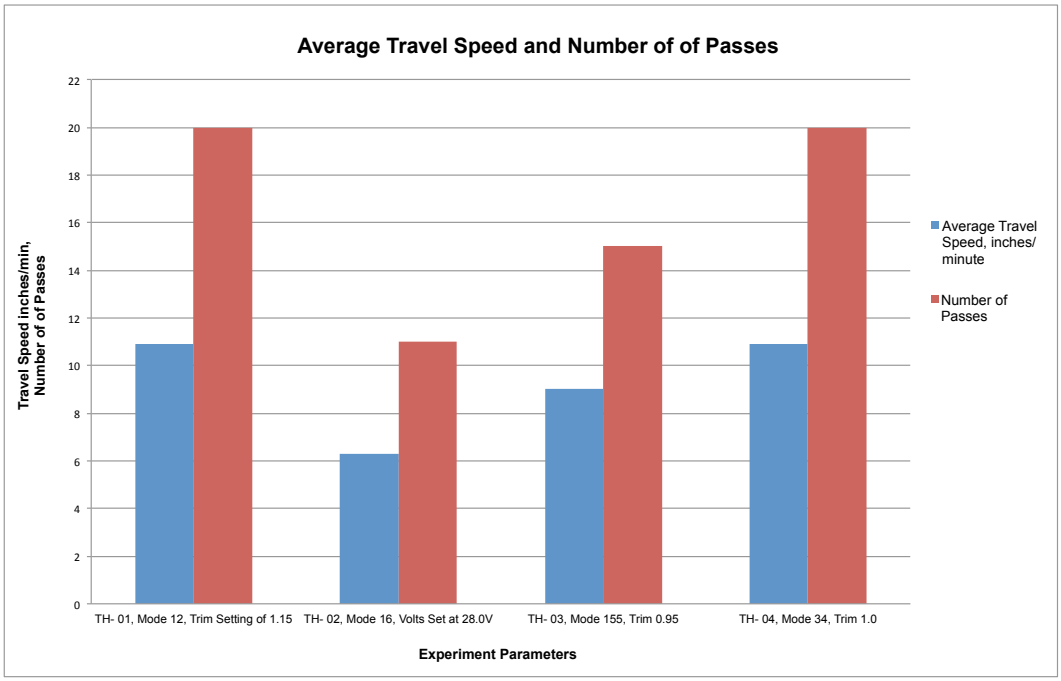

Figure 4.2 Graph of the Travel Speed and Number of Passes

By comparing the waveform's with the number of passes and travel speed a general bead profile can be determined. Looking at TH-01, TH-02, and TH-03's waveform and comparing it to TH-04's, significant variations exist. TH-04 is usually used to make stringer beads in duplex so as to reduce the amount of heat input placed into the base material. TH-04 and TH-01 both demonstrated the exact same number of passes.

4.2 Voltage vs. Time Waveform Analysis

Figure 4.3 shows the voltage waveforms attained from each experiment. As can be seen the average amount of voltage attained was similar between all tests,

indicating that welding conditions remained constant throughout the experiment. Has major difference occurred, it would have shown that temperature, humidity, or barometric pressure values had altered enough to alter the parameters necessary to weld.

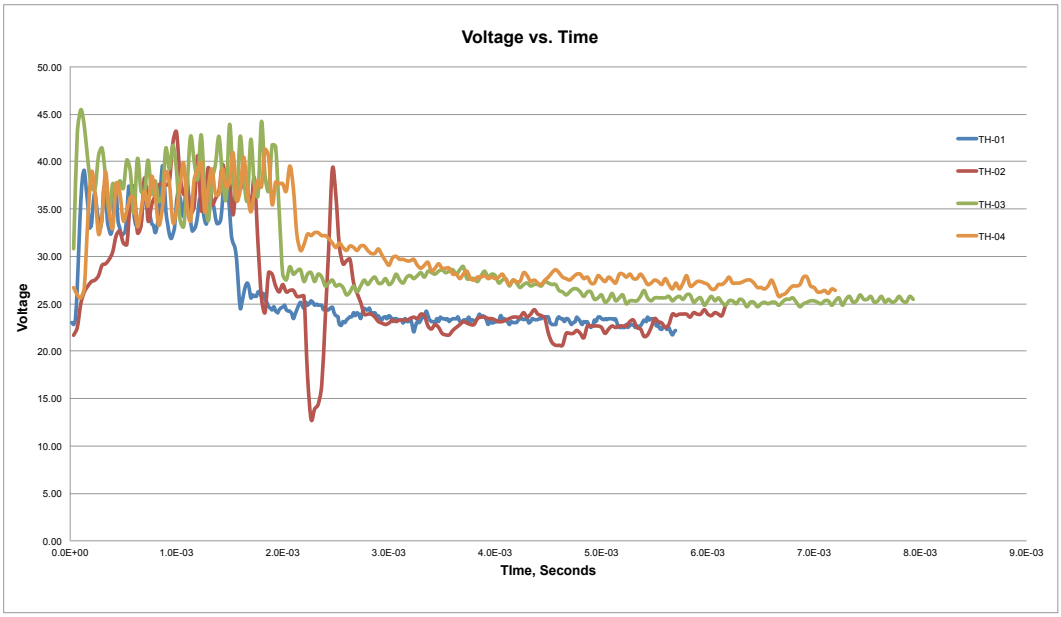

Figure 4.3 Voltage vs. Time Graph

4.3 Average Ultimate Tensile Strength and Average Yield Strength

Although the variation in waveforms were significant, they all produced an average ultimate tensile strength of 104-105 ksi, along with an average yield strength of 71-73 ksi; with all failures occurring in the base material. Table 4.1 below shows the average ultimate tensile strength, average yield strength, and location of failure for each experiment; it is arranged by increasing amounts of heat input.

Table 4.1 Tensile and Yield Strength Results

Experiment Number	Total Heat Input for Coupon	Average Ultimate Tensile Strength, Ksi	Average Yield Strength, Ksi	Location of Failure
TH- 02	504	105	73.0	Base Metal
TH- 04	550	104	71.1	Base Metal
TH- 03	625	105	72.1	Base Metal
TH- 01	635	105	72.9	Base Metal

Table 4.1 indicates a good matching of filler metal and base material, providing the welder a strong weld. It also shows that increased amounts of heat input coupled with waveform modification can allow for tensile strength to not be affected.

4.4 -40º Weld Metal and Heat Affected Zone Impact Results

Covered earlier, duplex is known for decreasing amounts of impact toughness with increasing amounts of heat input. Table 4.2 shows that with waveform modification, heat input can be increased, without negatively affecting impact toughness in both the weld metal and heat affected zone.

Table 4.2: -40º F impact toughness results

Experiment Number	Total Heat Input for Coupon	Average -40º Weld Metal Impact, ft-lbf	Average -40º Heat Affected Zone Impact, ft-lbf
TH- 02	504	69.0	110.7
TH- 04	550	48.0	41.7
TH- 03	625	70.5	86.0
TH- 01	635	70.0	41.0

All welds passed the 20 ft-lb minimum Westinghouse requirement for impact strength.

4.5 Percentage of Ferrite in the Weld Metal and Heat Affected Zone

The primary objective of these experiments was to find determine if waveform modification could affect the amount of ferrite content in a welded

joint. Table 4.3 shows average or "delta" the amount of ferrite present in the weld metal heat affected zone, and base material using ASTM E 562-08 Standard Test Methods for Detecting Volume Fraction by Systematic Manual Point Count. The weld metal, heat affected zone, and base material each had three samples taken, and then averaged.

Experiments TH-02, TH-03, and TH-04 had acceptable amounts of ferrite according to the Westinghouse document APP-VW20-Z0-023. However, TH-01 exceeded the 65% maximum limit, showing that this waveform should not be used for production welds.

Table 4.3 Delta Ferrite Results

Experiment Number	Total Heat Input for Coupon	% Delta Ferrite in the Weld Metal	% Delta Ferrite in the Heat Affected Zone	% Delta Ferrite in the Base Metal
TH- 02	504	46.0	54.0	45.0
TH- 04	550	43.0	60.0	49.0
TH- 03	625	50.0	50.0	48.0
TH- 01	635	47.0	70.0	47.0

Table 4.3 has been arranged by increasing amounts of heat input. It shows that ferrite content in the weld metal and base metal remains relatively constant as heat input increases.

The biggest changes in ferrite content come in the heat affected zone, with ferrite varying as much as 23% from the original amount present in the base metal. TH-02 had a 9% increase in ferrite and TH-04 had 11% increase but had the lowest amounts of heat input.

TH-03 had the smallest amount of change, 2%, in ferrite content in the heat affected zone, but had the third largest heat input. Experiment TH-03 also

demonstrated the same amount of ferrite in the heat affected zone as in the weld metal, indicating excellent dilution. This shows that acceptable higher amounts of heat input can be tolerated by duplex, along with meeting the Westinghouse requirement for ferrite.

The results attained from TH-04 show that with waveform medication and only a increase of 10 kJ/in ferrite can be increased as much as 23% over the base metal content.

Chapter 5

CONCLUSIONS & RECOMENDATIONS

Testing has indicated that the ferrite austenite phase balance of UNS-S32101 can be affected by wave-form modulation along with still being able to meet all of the standards set out by The American Welding Society and Westinghouse Electric Company. By increasing the ramp down rate of the wave-form, higher heat input values may be used instead of an overall lower heat input. By increasing the heat input, weldability and improved tie-in occurs. It was observed that contact tip degradation became higher as heat input increased due to spatter from the weld and reflected heat. This would cause replacement to occur every 2-3 layers.

Further research should be directed into determining at what ramp down rate UNS-S32101 begins to experience this increased ferrite with a at a heat input that is more welder friendly. This data should also be correlated with welder feedback in order to determine if there is a point where the weld pool solidifies too quickly inhibiting weld tie-in.

REFERENCES

E562 Volm Fraction by Point Count. In (2008). *Designation E 562 - 08* (pp. 1-7). ASTM International.

Ghosh, P., Dorn, L., Kulkarni, S., & Hofmann, F. (2008). Arc characteristics and behavior of metal transfer in pulsed current gma welding of stainless steel. In *Journal of Materials Processing Technology 209* (pp. 1-13).

Ghosh, P., Gupta, S., & Randhawa, H. (2000). Characteristics of a pulsed-current, vertical-up gas metal arc weld in steel. *Metallurgical and Materials Transactions. Part A, Physical Metallurgy and Materials Science*, *31A*(9), 2247-59. doi: 10.1007/s11661-000-0142-y

Joseph, A., Farson, D., Harwig, D., & Richardson, R. (2005). Influence of gmaw-p current waveform on heat input and weld bead shape. In *Science and Technology of Welding and Joining* (pp. 1-9). Columbus, OH: Maney.

Ldx 2101 fabrication. In *UNS S32101* (pp. 1-12). Temperance, MI: Rolled Alloys.

Sieurin, H., Sandström, R., & Westin, E. (2006). Fracture Toughness of the Lean Duplex Stainless Steel LDX 2101. *Metallurgical and Materials Transactions. Part A, Physical Metallurgy and Materials Science*, *37A*(10), 2975-81. doi: 10.1007/s11661-006-0179-7

Practical Guidelines for the Fabrication of Duplex Stainless Steel. In (2009). *TMR Stainless* London, UK: International Molybdenum.

Process: Pulsed spray metal transfer. In (2004). *Lincoln Electric.* Lincoln Global, Inc. Retrieved from http://www.treatrade.hr/pdf/DM/psmt.pdf

Nextweld: True energy. In (2009). *Lincoln Electric* (pp. 1-4). Lincoln Global, Inc.

Norrish, J. (2006). Advanced welding processes: Technologies and process control. Cambridge, England: Woodhead Publishing Limited.

Smith, W. (2011). Welding specification for astm a240 uns s32101 duplex stainless steel plate. In *APP-VW20-Z0-023_2* (pp. 1-16). Westinghouse.

Standard test methods and definitions for mechanical testing of steel products. In (2009). *Designation A370 - 09a* ASTM International.

APPENDIX A

RAW DATA ATTAINED FROM PROCESS QUALIFICTION REPORT

Test Plate #1, Mode 12, Trim Setting of 1.15									
Pass #	Amps		Volts		Wire Feed Speed,	Interpass Temperature, Degrees Fahrenheit	Travel Speed, inches/minute	True Energy, kJ	Heat Input, kJ/inch
	Min	Max	Min	Max					
1	148	170	27.3	28.1	400	79	11.4	303	25.3
2	140	180	27.7	28.3	400	261	7.3	482	40.2
3	154	184	27.4	28.3	400	88	9.1	419	34.9
4	164	184	27.4	28.0	400	370	12.0	304	25.3
5	159	204	27.4	28.0	400	242	9.7	380	31.7
6	148	183	27.6	28.6	400	492	9.4	368	30.7
7	138	180	27.6	28.0	400	283	9.6	382	31.8
8	152	220	27.1	27.4	400	446	10.0	279	23.3
9	153	168	27.4	28.0	400	275	11.8	301	25.1
10	138	160	27.6	28.0	400	468	12.6	268	22.3
11	168	192	27.6	28.0	400	502	11.4	328	27.3
12	153	170	27.5	28.5	400	522	7.7	450	37.5
13	162	182	27.5	28.5	390	367	12.9	282	23.5
14	136	163	27.0	27.9	390	276	14.1	229	19.1
15	136	178	27.5	27.8	390	427	14.4	256	21.3
16	158	173	27.4	27.8	390	480	12.6	285	23.8
17	142	151	27.3	27.8	390	492	12.4	262	21.8
18	132	147	27.3	27.9	390	514	12.9	252	21.0
19	132	160	27.2	27.9	390	406	8.1	385	32.1
20	131	161	27.3	28.0	390	140	8.0	387	32.3
						Max	**14.4**	**482**	**40.2**
						Min	**7.3**	**229**	**19.1**
						Average	**10.9**	**330**	**27.5**
							Total	**6602**	**550**

Test Plate #2, Mode 16, Volts Set at 28.0V									
Pass #	Amps		Volts		Wire Feed Speed, inches/minute	Interpass Temperature, Degrees Fahrenheit	Travel Speed, inches/minute	True Energy, kJ	Heat Input, kJ/inch
	Min	Max	Min	Max					
1	131	150	27.7	28.7	375	67	8.1	398	33.2
2	128	160	27.9	28.6	375	262	6.2	524	43.7
3	148	212	28.6	29.2	375	335	7.1	514	42.8
4	118	140	27.6	28.6	375	402	4.3	722	60.2
5	127	172	27.2	29.0	375	479	7.3	489	40.8
6	130	148	27.9	28.6	375	388	10.0	325	27.1
7	126	153	27.9	28.6	375	435	6.6	478	39.8
8	128	156	27.9	28.6	375	319	6.1	521	43.4
9	119	144	27.7	28.5	375	351	4.4	702	58.5
10	129	150	27.8	28.6	375	398	5.4	694	57.8
11	112	141	27.8	28.5	375	411	4.4	690	57.5
						Max	**10.0**	**722**	**60.2**
						Min	**4.3**	**325**	**27.1**
						Average	**6.3**	**551**	**45.9**
							Total	**6057.0**	**504.8**

Test Plate #3, Mode 155, Trim 0.95									
Pass #	Amps		Volts		Wire Feed Speed,	Interpass Temperature,	Travel Speed,	True Energy,	Heat Input,
	Min	Max	Min	Max	inches/minute	Degrees Fahrenheit	inches/minute	kJ	kJ/inch
1	146	147	28.7	31.1	350	76	6.9	527	43.9
2	154	155	25.4	30	400	215	7.9	442	36.8
3	143	195	25.3	33.7	400	351	5.8	709	59.1
4	148	179	24.7	30.7	380	325	6.6	569	47.4
5	117	232	24.3	31.9	400	412	5.2	828	69.0
6	164	170	26.3	30.7	400	389	4.7	825	68.8
7	167	168	27.8	30.6	400	423	10.1	395	32.9
8	142	222	23.4	33.1	400	300	12.2	336	28.0
9	165	168	27.7	32.7	400	111	12.0	342	28.5
10	166	167	29.3	31	400	400	5.9	694	57.8
11	162	173	26.3	31.3	400	527	15.3	257	21.4
12	167	184	27.6	29	400	502	13.8	288	24.0
13	153	189	26.1	30.8	400	491	10.4	389	32.4
14	154	187	25.7	31.4	400	217	9.9	401	33.4
15	155	185	25.8	31.4	400	394	7.8	499	41.6
						Max	**15.3**	**828**	**69.0**
						Min	**4.7**	**257**	**21.4**
						Average	**9.0**	**500**	**41.7**
							Total	**7501.0**	**625.1**

Test Plate #4, Mode 34, Trim 1.0									
Pass #	Amps		Volts		Wire Feed Speed, inches/minute	Interpass Temperature, Degrees Fahrenheit	Travel Speed, inches/minute	True Energy, kJ	Heat Input, kJ/inch
	Min	Max	Min	Max					
1	131	213	29.2	29.6	375	78	9.7	422	35.2
2	129	171	28.9	30	375	241	6.9	499	41.6
3	112	209	28.5	30.3	375	362	8.6	448	37.3
4	100	222	28.3	30.5	375	381	8.4	440	36.7
5	111	217	28.4	30.4	375	422	14.4	271	22.6
6	144	223	30.3	30.6	375	483	6.2	504	42.0
7	105	249	29.4	31.4	375	566	8.3	666	55.5
8	117	265	28.9	31.8	375	491	8.3	560	46.7
9	136	250	29.2	31.6	375	414	17.1	258	21.5
10	134	251	29.1	31.6	375	553	10.9	402	33.5
11	126	256	29.1	31.6	375	532	9.2	460	38.3
12	160	215	29.1	29.6	370	489	9.1	403	33.6
13	121	259	29.1	31.7	410	567	8.4	515	42.9
14	120	246	28.9	31.3	350	308	11.3	276	23.0
15	122	237	28.8	31.0	350	501	12.4	278	23.2
16	123	229	28.7	30.7	350	534	13.6	244	20.3
17	140	173	28.2	28.7	350	545	12.9	276	23.0
18	122	222	28.7	30.5	350	547	11.6	270	22.5
19	122	217	28.6	30.4	350	561	16.4	194	16.2
20	122	212	28.6	30.3	350	501	13.6	233	19.4
						Max	**17.1**	**666**	**55.5**
						Min	**6.2**	**194**	**16.2**
						Average	**10.9**	**381**	**31.7**
							Total	**7619.0**	**634.9**

APPENDIX B

GRAPHS AMPS VERSUS TIME

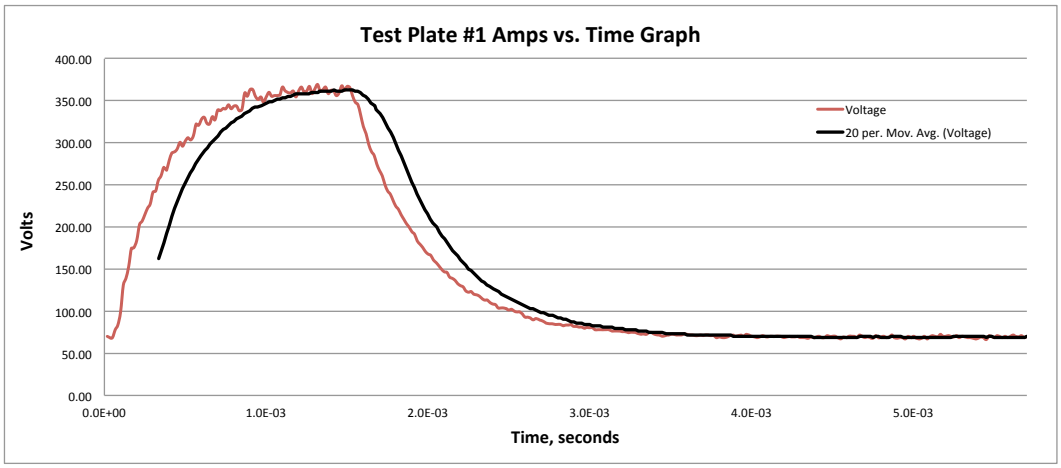
Test Plate #1 Amps vs. Time Graph
400.00
350.00
300.00
250.00
200.00
150.00
100.00
50.00
0.00
Volts
0.0E+00
1.0E-03
2.0E-03
3.0E-03
4.0E-03
5.0E-03
Time, seconds
Voltage
20 per. Mov. Avg. (Voltage)

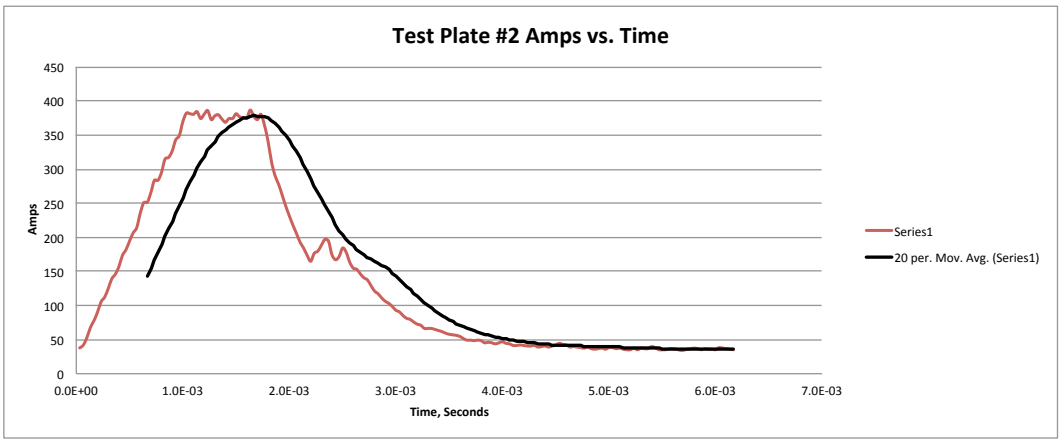
Test Plate #2 Amps vs. Time
450
400
350
300
250
200
150
100
50
0
Amps
0.0E+00
1.0E-03
2.0E-03
3.0E-03
4.0E-03
5.0E-03
6.0E-03
7.0E-03
Time, Seconds
Series1
20 per. Mov. Avg. (Series1)

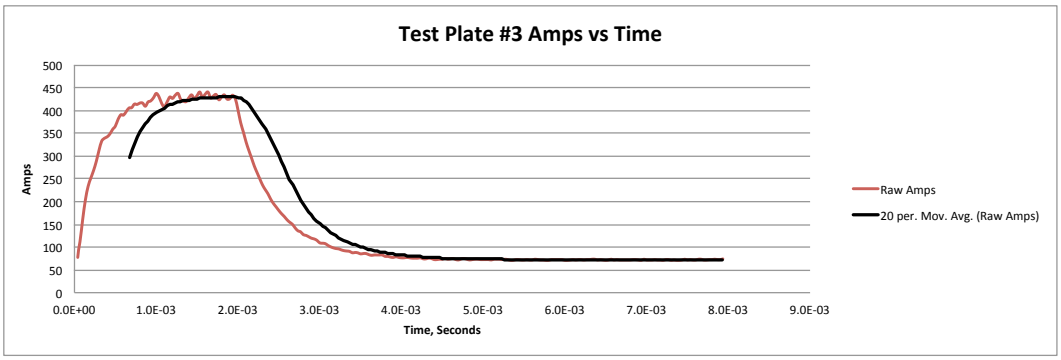
Test Plate #3 Amps vs Time
Amps
500
450
400
350
300
250
200
150
100
50
0
0.0E+00
1.0E-03
2.0E-03
3.0E-03
4.0E-03
5.0E-03
6.0E-03
7.0E-03
8.0E-03
9.0E-03
Time, Seconds
Raw Amps
20 per. Mov. Avg. (Raw Amps)

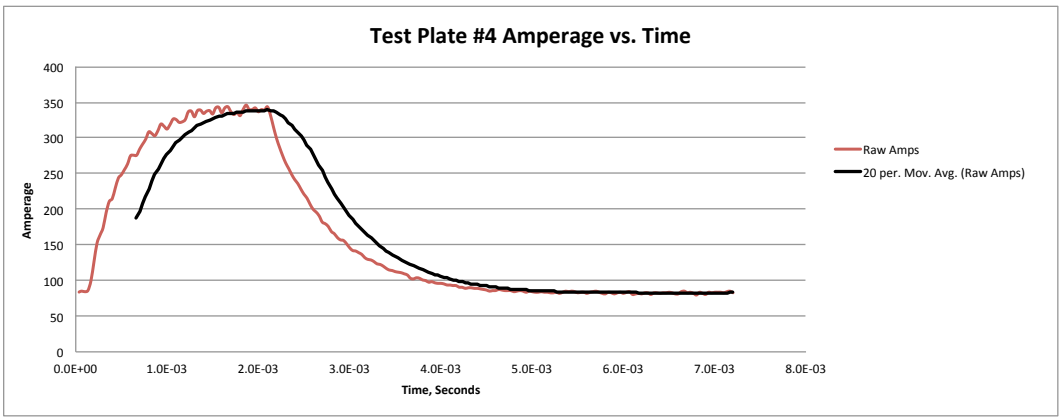
Test Plate #4 Amperage vs. Time
Amperage
400
350
300
250
200
150
100
50
0
0.0E+00
1.0E-03
2.0E-03
3.0E-03
4.0E-03
5.0E-03
6.0E-03
7.0E-03
8.0E-03
Time, Seconds
Raw Amps
20 per. Mov. Avg. (Raw Amps)

APPENDIX C

GRAPHS VOLTS VERSUS TIME

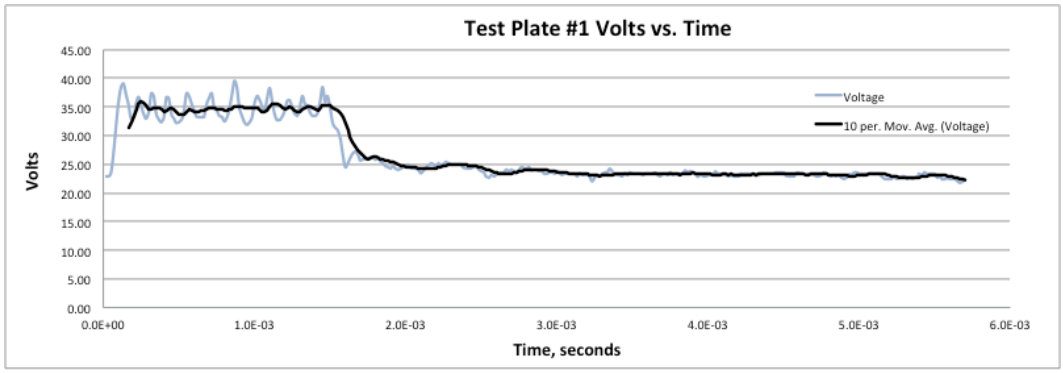
Test Plate #1 Volts vs. Time
Volts
45.00
40.00
35.00
30.00
25.00
20.00
15.00
10.00
5.00
0.00
0.0E+00
1.0E-03
2.0E-03
3.0E-03
4.0E-03
5.0E-03
6.0E-03
Time, seconds
Voltage
10 per. Mov. Avg. (Voltage)

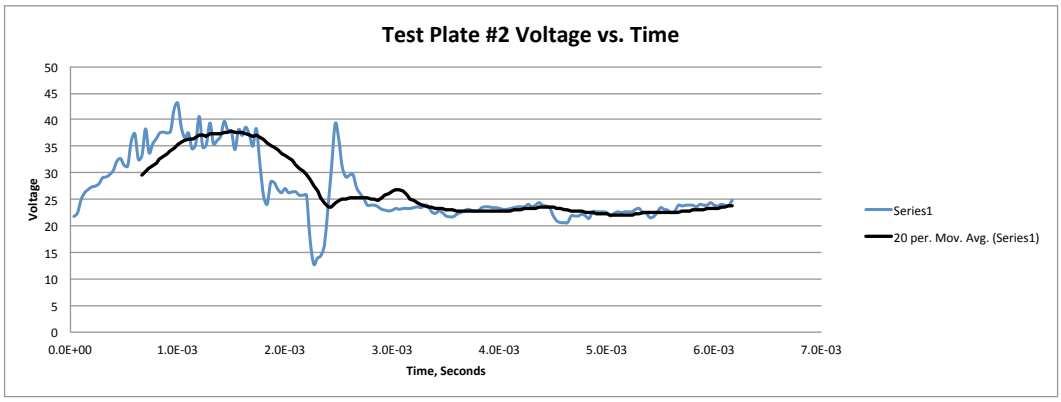
Test Plate #2 Voltage vs. Time
Voltage
50
45
40
35
30
25
20
15
10
5
0
0.0E+00
1.0E-03
2.0E-03
3.0E-03
4.0E-03
5.0E-03
6.0E-03
7.0E-03
Time, Seconds
Series1
20 per. Mov. Avg. (Series1)

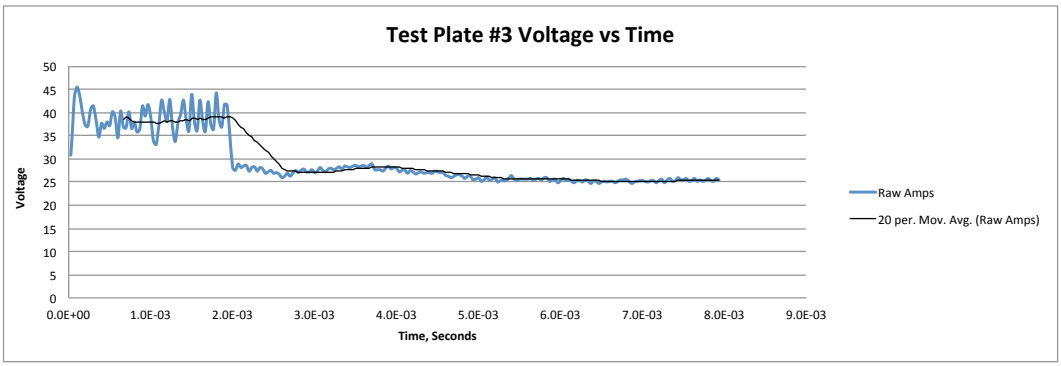
Test Plate #3 Voltage vs Time
Voltage
50
45
40
35
30
25
20
15
10
5
0
0.0E+00
1.0E-03
2.0E-03
3.0E-03
4.0E-03
5.0E-03
6.0E-03
7.0E-03
8.0E-03
9.0E-03
Time, Seconds
Raw Amps
20 per. Mov. Avg. (Raw Amps)

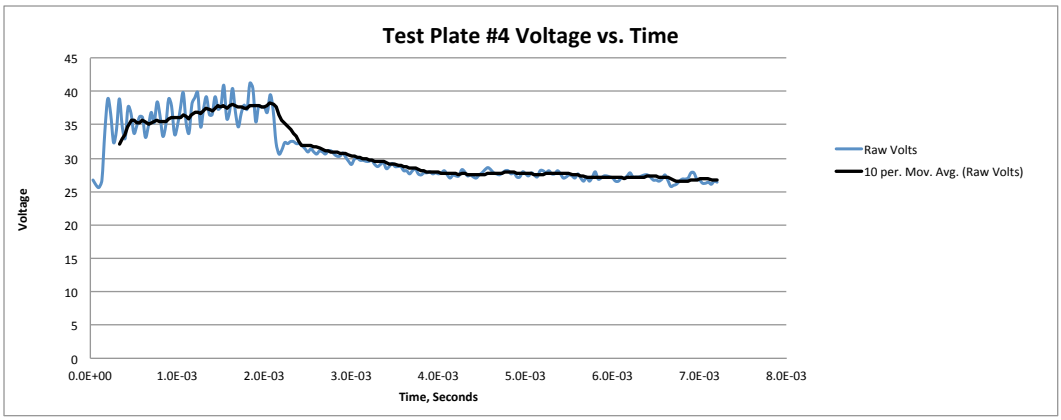
Test Plate #4 Voltage vs. Time
Voltage
45
40
35
30
25
20
15
10
5
0
0.0E+00
1.0E-03
2.0E-03
3.0E-03
4.0E-03
5.0E-03
6.0E-03
7.0E-03
8.0E-03
Time, Seconds
Raw Volts
10 per. Mov. Avg. (Raw Volts)